

Damping of supernova neutrino transitions in stochastic shock-wave density profiles

Gianluigi Fogli, Eligio Lisi, Alessandro Mirizzi

Dipartimento di Fisica and Sezione INFN di Bari
Via Amendola 173, 70126 Bari, Italy

Daniele Montanino

Dipartimento di Fisica and Sezione INFN di Lecce
Via Arnesano, 73100 Lecce, Italy

Abstract. Supernova neutrino flavor transitions during the shock wave propagation are known to encode relevant information not only about the matter density profile but also about unknown neutrino properties, such as the mass hierarchy (normal or inverted) and the mixing angle θ_{13} . While previous studies have focussed on “deterministic” density profiles, we investigate the effect of possible stochastic matter density fluctuations in the wake of supernova shock waves. In particular, we study the impact of small-scale fluctuations on the electron (anti)neutrino survival probability, and on the observable spectra of inverse-beta-decay events in future water-Cherenkov detectors. We find that such fluctuations, even with relatively small amplitudes, can have significant damping effects on the flavor transition pattern, and can partly erase the shock-wave imprint on the observable time spectra, especially for $\sin^2 \theta_{13} \gtrsim \mathcal{O}(10^{-3})$.

PACS numbers: 14.60.Pq, 97.60.Bw, 02.50.Ey

1. Introduction

Future observations of supernova (SN) neutrinos in underground detectors represent a subject of intensive investigation in astroparticle physics. In this context, matter effects associated to neutrino flavor transitions in the SN envelope have been widely studied as a unique tool to probe, at the same time, neutrino properties and supernova astrophysics (see, e.g. [1–4] for recent reviews). In particular, the effects of supernova shock waves on neutrino flavor transitions in matter [5] are gaining increasing attention in the recent literature [6–11]. Indeed, for a few seconds after the SN core bounce, the strong time dependence of the shock-wave profile can leave peculiar signatures on the time structure of the neutrino events, which could be monitored in large, real-time detectors [12–14].

So far, studies of supernova neutrino flavor transitions during the shock-wave propagation have been based on “deterministic” matter density profiles, assumed to be known (or at least knowable, in principle) both in time and in radial dependence. However, stochastic density fluctuations and inhomogeneities, of various magnitudes and correlation lengths, may reasonably arise in the wake of a shock front. Possible causes of these inhomogeneities include microscopic fluctuations in the nascent neutron star [15] and large-scale fluctuations between the proto-neutron star and the supernova envelope due to hydrodynamical instabilities [16–18]. At early times ($\lesssim 1$ s after bounce), post-shock convection overturns can also produce large density anisotropies. A supernova neutrino “beam” traveling to the Earth might thus experience stochastic matter effects while traversing the stellar envelope.

Concerning neutrino oscillations, the phenomenology of possible stochastic matter density fluctuations has been investigated in several contexts, with emphasis on general properties [19–22] and on the solution to the solar neutrino problem [23–28]. Supernova neutrinos have specifically been considered in relatively few cases [29], and only for a *static* profile. In general, it is found that the typical effect of random fluctuations on neutrino oscillations is to wash out the phase information (if any) and to damp the flavor transition pattern in the energy domain. It seems thus worthwhile to revisit this topic in the context of *dynamic* SN density profiles, which offer a complementary handle in the time domain.‡ Moreover, stochastic density fluctuations are expected to arise more easily in the wake of a SN shock wave than in a relatively static stellar environment.

In this work we try to explore quantitatively the entangled effects of shock waves and of possible stochastic fluctuations (behind the shock front) on supernova neutrino flavor transition probabilities and observables. Unfortunately, current core-collapse SN simulations do not yet offer a clear input for such phenomena, both because the details of the explosion mechanism are not well understood yet, and because current computer resources do not allow to resolve density variations at scales smaller than, say, $O(10)$ km. Therefore, some assumptions and simplifications are unavoidable. In particular, we shall limit ourselves to small-scale and small-amplitude fluctuations, which are definitely not excluded by current simulations, and which allow a simple perturbative approach.

‡ This possibility was mentioned in passing in the seminal Ref. [5].

Our work is organized as follows. In Section 2 we introduce the notation for the neutrino mass and mixing parameters and for the electron (anti)neutrino survival probability P_{ee} characterizing supernova neutrino transitions. In Section 3 we parametrize the “fluctuating” shock-wave profile and discuss an approximate analytic expression for the survival probability P_{ee} , which neatly includes the damping effect induced by density fluctuations. In particular, the analytical derivation of P_{ee} from the neutrino master equation for the density matrix, together with a comparison with representative numerical solutions, are given in the Appendix. We find that, for $\sin^2 \theta_{13} \gtrsim \mathcal{O}(10^{-3})$, small-scale stochastic fluctuations can suppress the imprint of the shock wave on the flavor transition pattern in the time domain. In Section 4 we discuss a specific experimental application for the case of antineutrinos in inverted hierarchy, by calculating the effects of fluctuations on positron event spectra observable in water-Cherenkov detectors through inverse beta decay. Conclusions and prospects for further developments are given in Section 5. The bottom line of our work is that some “smearing” of shock-wave signatures in neutrino observables is to be expected, if stochastic matter fluctuations are present in the wake of the shock front. Improvements in supernova hydrodynamical simulations will greatly help to clarify this issue.

2. Three-neutrino mixing framework

In this section we set the notation for three-neutrino mixing and for the survival probability of electron (anti)neutrinos P_{ee} . In the current “standard” 3ν scenario, the dominant parameters relevant to flavor transitions in supernovae are the largest squared mass difference Δm^2 and the mixing angles θ_{12} and θ_{13} (see, e.g., [30, 31]). In numerical examples, we take as reference values (close to their best fits [32])

$$\Delta m^2 \simeq 2.4 \times 10^{-3} \text{ eV}^2, \quad (1)$$

$$\sin^2 \theta_{12} \simeq 0.3. \quad (2)$$

The sign of Δm^2 distinguishes the cases of normal hierarchy (NH: $+\Delta m^2$) and inverted hierarchy (IH: $-\Delta m^2$). Concerning the mixing parameter $\sin^2 \theta_{13}$, we shall use representative values below the current upper limits ($\sin^2 \theta_{13} < \text{few} \times 10^{-2}$ [33]).

The smallest squared mass difference ($\delta m^2 \simeq 8 \times 10^{-5} \text{ eV}^2$ [32]) is such that $\delta m^2 / \Delta m^2 \ll 1$; together with the smallness of $\sin^2 \theta_{13}$, this fact guarantees, to a very good approximation, the factorization of the 3ν dynamics into a “low” (L) and a “high” (H) 2ν subsystem. In other words, the electron (anti)neutrino survival probability P_{ee} , up to small terms of $\mathcal{O}(\sin^2 \theta_{13}, \delta m^2 / \Delta m^2)$, can be expressed as

$$P_{ee} \simeq P_{ee}^L \cdot P_{ee}^H, \quad (3)$$

where P_{ee}^L and P_{ee}^H represent effective electron (anti)neutrino survival probabilities in the 2ν subsystems (see [30, 31, 34–36] and references therein).

Neglecting Earth matter effects (not included in this work), one has [8, 30, 31]

$$P_{ee}^L \simeq \begin{cases} \sin^2 \theta_{12} & (\text{for } \nu, \text{ any hierarchy}), \\ \cos^2 \theta_{12} & (\text{for } \bar{\nu}, \text{ any hierarchy}), \end{cases} \quad (4)$$

and

$$P_{ee}^H \simeq \begin{cases} P_+^H & (\text{for } \nu \text{ in NH or } \bar{\nu} \text{ in IH}), \\ P_-^H & (\text{for } \bar{\nu} \text{ in NH or } \nu \text{ in IH}), \end{cases} \quad (5)$$

where P_{\pm}^H are defined below.

In general, P_{ee}^H depends on θ_{13} , on the hierarchy, and on the wavenumber k_H in the H subsystem,

$$\pm k_H = \pm \Delta m^2 / 2E \quad (+ \text{ for NH, } - \text{ for IH}), \quad (6)$$

and on the (anti)neutrino potential in matter [37],

$$\pm V(x) = \pm \sqrt{2} G_F N_e(x) \quad (+ \text{ for } \nu, - \text{ for } \bar{\nu}) \quad (7)$$

where N_e is the electron density at the supernova radius x .

Strong matter effects are generally expected when the “level crossing condition”

$$\pm k_H \simeq \pm V(x_c) \quad (\text{for } \nu \text{ in NH or } \bar{\nu} \text{ in IH}), \quad (8)$$

is satisfied at (more than) one point x_c (see [31]). The crossing condition requires equal signs for V and k_H , so it is not realized for $\bar{\nu}$ in NH or ν in IH. The physics of matter effects can be encoded in terms of the so-called crossing probability P_c [30, 38]

$$P_c = \begin{cases} P_c(k_H, \sin^2 \theta_{13}, V) & (\text{for } \nu \text{ in NH or } \bar{\nu} \text{ in IH}), \\ \sim 0 & (\text{for } \bar{\nu} \text{ in NH or } \nu \text{ in IH}), \end{cases} \quad (9)$$

where $P_c \neq 0$ ($=0$) defines the case of nonadiabatic (adiabatic) matter transitions. §

In the standard case (with no stochastic fluctuations) the survival probability P_{\pm}^H at the Earth (averaged over many oscillation cycles) is related to the crossing probability P_c through the well-known Parke’s formula [44],

$$P_{\pm}^H \simeq \frac{1}{2} + \left(\frac{1}{2} - P_c \right) \cos 2\theta_{13} \cos 2\tilde{\theta}_{13}^{\pm}(x_0) \quad (\text{no fluctuations}), \quad (10)$$

where x_0 is the neutrino production point, and

$$\cos 2\tilde{\theta}_{13}^{\pm}(x) = \frac{\cos 2\theta_{13} \mp V(x)/k_H}{\sqrt{(\cos 2\theta_{13} \mp V(x)/k_H)^2 + (\sin 2\theta_{13})^2}}, \quad (11)$$

defines the mixing angle $\tilde{\theta}_{13}^{\pm}$ in matter. In Eq. (11), the upper and lower signs correspond to the upper and lower signs of P_{\pm}^H in Eq. (5). Due to the high matter density at the origin ($|V(x_0)/k_H| \gg 1$), in Eq. (10) one can simply put

$$\cos 2\tilde{\theta}_{13}^{\pm}(x_0) \simeq \mp 1. \quad (12)$$

A final remark is in order. In the presence of density fluctuations with small amplitude, one does not expect that the crossing probability P_c is significantly perturbed, being related to a “local” nonadiabatic effect. The relation between P_{\pm}^H and

§ Concerning the early literature on two-level crossings, it is amusing to note that the classic Landau-Zener-Stückelberg results for P_c [39–41] were similarly obtained by Majorana [42] in the context of spin-flip transitions in variable magnetic fields, see the discussion in [43]. Curiously, this contribution by Majorana (well known in atomic physics) is largely ignored in the neutrino literature.

P_c in Eq. (10) is instead expected to change, being related to the “global” propagation history within the supernova matter. This intuitive picture, which enters in the analytical generalization of Eq. (10) discussed in the next section, is confirmed by numerical calculations (see the Appendix). Similarly, one does not expect that small-amplitude fluctuations can ruin the effective $L \otimes H$ factorization, which relies only on the smallness of θ_{13} and of $\delta m^2/\Delta m^2$. This expectation is also supported by the smallness of fluctuation effects within the L subsystem in our framework (see the last paragraph in Sec. 3.3). A full numerical confirmation of the $L \otimes H$ factorization in the presence of stochastic effects, however, would involve rather heavy calculations of exact 3ν solutions, which are beyond the scope of this work.

3. Effects of stochastic matter fluctuations on SN neutrino transitions

In this Section we parametrize the SN stochastic density fluctuations through some simplifying assumptions (Sec. 3.1), characterize their effects through an analytical prescription for the calculation of the probability P_{\pm}^H (Sec. 3.2), and discuss the time dependence of P_{\pm}^H in the presence of fluctuations with increasing amplitude (Sec. 3.3).

3.1. Shock-wave density profile and stochastic fluctuations

We make the reasonable assumption that stochastic fluctuations arise only *after* the passage of the shock-wave. Behind the shock front, fluctuations can be described as fractional (random) variations $\xi(x)$ of an “average” neutrino potential V_0 ,

$$V(x) = V_0(x) + \delta V(x) = V_0(x)[1 + \xi(x)] , \quad (13)$$

with vanishing mean $\langle \xi(x) \rangle = 0$, and with variance $\xi^2 = \langle \xi(x)^2 \rangle$. In the absence of further information, we simply assume that ξ is both constant and small [$O(\text{few}\%)$].^{||}

We also assume that the fluctuations arise at relatively small length scales L_0 , as compared with the neutrino oscillation length in matter λ_m . In the region where matter effects are relevant ($V \simeq k_H$), this condition reads:

$$\begin{aligned} L_0 \ll \lambda_m &\simeq \frac{2\pi}{k_H \sin 2\theta_{13}} \\ &\simeq 60 \text{ km} \left(\frac{E}{10 \text{ MeV}} \right) \left(\frac{2 \times 10^{-3} \text{ eV}^2}{\Delta m^2} \right) \left(\frac{0.2}{\sin 2\theta_{13}} \right) . \end{aligned} \quad (14)$$

In all numerical examples we shall assume a representative value

$$L_0 \simeq 10 \text{ km} . \quad (15)$$

Notice that this scale is of the same order as the radial hydrodynamical fluctuations described in [15], as well as of the neutrinosphere radius [1], which sets the transverse size of the SN neutrino beam in the Earth direction.

^{||} In a different context (Sun density profile), the combination of all available solar and KamLAND data sets an upper limit $\xi < 5\%$ at 70 % CL for the solar density fluctuations, assuming a fluctuation length scale $L_0 = 10 \text{ km}$ [28].

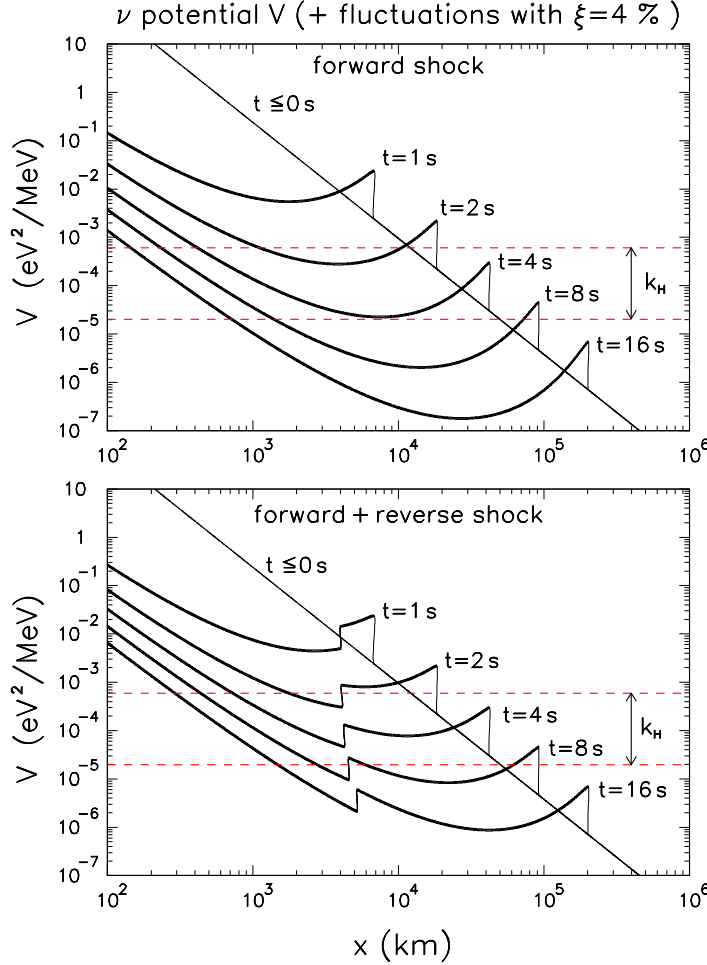


Figure 1. Simplified radial profiles of the neutrino potential $V(x)$ at different post-bounce times t (1, 2, 4, 8, and 16 s). The thicker curves behind the shock front represent fluctuations of amplitude $\xi \leq 4\%$ of the local matter potential V . Upper panel: Forward shock only. Lower panel: Forward plus reverse shock. In both cases, the static (pre-bounce) profile ($t \leq 0$ s) is also shown. The band within dashed lines marks the region where SN matter effects are potentially important ($V \simeq k_H$, with $E = 2\text{--}60$ MeV).

The small-scale assumption in Eqs. (14) and (15) implies that the autocorrelation function of the random field $\xi(x)$ can be written as an effective delta-function [20–23]

$$\langle \xi(x_1) \xi(x_2) \rangle = 2L_0 \xi^2 \delta(x_1 - x_2) . \quad (16)$$

In a nutshell, fluctuations between points much closer (much farther) than one neutrino oscillation length in matter are assumed to be fully correlated (totally uncorrelated). Given Eq. (16), the master equation for the neutrino flavor evolution is determined (see the Appendix).

Figure 1 shows the (fluctuating) shock-wave profiles used in this work. We take the unperturbed shock-wave potentials $V_0(x)$ from our previous simplified parametrizations in [8, 12]. In the region behind the shock front, the thicker curves

represent a band of fluctuations with fractional deviation $\xi \leq 4\%$. The upper panel refers to the neutrino potential V in the presence of the forward shock only. In the lower panel we have taken into account also a possible reverse shock, characterized by a smaller density jump at the front [9]. In both panels, we also show the band spanned by the neutrino wavenumber $k_H = \Delta m^2/2E$ for $E \in [2, 60]$ MeV. Notice that the (crossing) condition for large matter effects ($V \simeq k_H$) is basically unperturbed by fluctuations as small as those in Fig. 1.

3.2. Analytical results

As anticipated in Sec. 2, the survival probability P_{\pm}^H in the H subsystem is modified by matter density fluctuations. In general, the calculation of P_{\pm}^H requires that the stochastic master equation (see Appendix) is solved numerically. Nevertheless, as shown in [24] and described in detail in the Appendix, small-scale and small-amplitude fluctuations allow to use perturbative techniques which, already at first order, provide rather accurate analytical approximations. In the context of SN neutrinos, the analytical prescription reads

$$P_{\pm}^H \simeq \frac{1}{2} \mp \left(\frac{1}{2} - P_c \right) e^{-\Gamma_{\pm}} \cos 2\theta_{13} , \quad (17)$$

which generalizes [24] Parke's formula (10) [in the conditions of Eq. (12)] through a simple exponential damping factor $e^{-\Gamma_{\pm}}$, whose exponent is given by

$$\Gamma_{\pm} = \int_{x_0}^{x_s} \mathcal{D}(x) \sin^2 2\tilde{\theta}_{13}^{\pm}(x) dx , \quad (18)$$

where

$$\mathcal{D}(x) = \xi^2 V_0^2(x) L_0 , \quad (19)$$

and the mixing angle in matter ($\tilde{\theta}_{13}^{\pm}$) is defined as in Eq. (11). The domain of the damping integral Γ_{\pm} is the region behind the forward shock front position x_s , where stochastic fluctuations are assumed to arise. For strong damping ($\Gamma_{\pm} \gg 1$) one gets the limit $P_{\pm}^H \rightarrow 1/2$, corresponding to a sort of complete ‘‘flavor depolarization,’’ where the two effective ν states in the H subsystem are democratically mixed.

All stochastic matter effects are embedded in the damping factor $e^{-\Gamma_{\pm}}$, while the crossing probability $P_c = P_c(k_H, \sin^2 \theta_{13}, V(x))$ in Eq. (17) is basically unperturbed.¶ In particular, P_c can be evaluated analytically by considering the ordered product of crossing matrices along the average (nonmonotonic) supernova shock-wave density profile $V_0(x)$, as previously discussed in [8, 12]. Therefore, apart from the numerical evaluation of the integral in Eq. (18), P_{\pm}^H can be computed through convenient analytical approximations.

¶ This fact is also verified a posteriori through the very good agreement of the analytical recipe in Eq. (17) with the numerical solution, as shown in the Appendix. The check is nontrivial, since the accuracy of the analytical approximation in Eq. (17), discussed in [24] in the context of the (static and monotonic) solar matter profile, cannot be taken for granted in the (dynamic and nonmonotonic) supernova profile.

3.3. Analysis of the survival probability P_{\pm}^H in the H subsystem, and comments on P_{ee}^L in the L subsystem

In this Section we describe the behaviour of P_{\pm}^H as a function of time, in the presence of stochastic fluctuations with increasing amplitude ξ . The case of no fluctuations is recovered for $\xi = 0$.

Figure 2 shows the variations of the survival probability P_+^H (relevant for ν in NH or $\bar{\nu}$ in IH),

$$P_+^H \simeq \frac{1}{2} - \left(\frac{1}{2} - P_c\right) e^{-\Gamma_+ \cos 2\theta_{13}} , \quad (20)$$

in the time interval $t \in [1, 13]$ s, for $\xi = 0$ (solid curves), $\xi = 2\%$ (dashed curves) and $\xi = 4\%$ (dotted curves). The neutrino energy is fixed at $E = 30$ MeV, while $\sin^2 \theta_{13}$ ranges from 10^{-2} (upper panels) to 10^{-5} (lower panels). We include both the case of forward shock only (left panels) and of forward plus reverse shock (right panels).

In the absence of fluctuations, the function $P_+^H(t)$ in Fig. 2 shows strong, nonmonotonic variations: A clear signature of the strongly nonadiabatic flavor transitions along the shock front, operative in the time window $t \in \sim [3, 9]$ s (as discussed at length in [8, 12]). In the presence of stochastic fluctuations behind the shock front, however, the variations are partly suppressed, as a result of the “flavor depolarization” effect. As the amplitude ξ increases, the survival probability P_+^H gets closer to the saturation value $1/2$. The effect of fluctuations is relevant in the same time window where shock effects are operative, since the occurrence of the condition $V \simeq k_H$ (in multiple points x_c) leads to $\sin^2 2\tilde{\theta}_{13}^+ \simeq 1$ and thus to a “large” damping factor [see Eq. (18)] around x_c . At earlier or later times, the enhancement of θ_{13} in matter is more modest and so are fluctuation effects.

In Fig. 2, the smearing effect of fluctuations appears to be particularly dangerous for the identification of shock-wave signatures: For instance, for $\xi = 4\%$, the double-peak structure associated to the forward+reverse shock (right panels) may be washed out, becoming more similar to the case of forward shock only (left panels). A “confusion scenario” might arise, limiting the potential to monitor the shock-wave propagation through neutrino flavor transitions.

Figure 2 also shows that, in general, damping effects are suppressed at small values of θ_{13} (say, $\sin^2 \theta_{13} \lesssim 10^{-3}$). This fact can be understood by expanding the damping integral [Eq. (18)] around the crossing points x_c , where the integrand is locally maximal. At first order in $x - x_c$, and using the fact that $V \simeq k_H$ around x_c , one gets then

$$\Gamma_+ \simeq \pi \sin 2\theta_{13} \sum_{x_c} \mathcal{D}(x_c) \left| \frac{d \ln V}{dx} \right|_{x_c}^{-1} , \quad (21)$$

which shows that the damping factor is basically proportional to θ_{13} . In conclusion, for values of $\sin^2 \theta_{13} \gtrsim \mathcal{O}(10^{-3})$, small-scale stochastic fluctuations with a fractional amplitude of a few percent might significantly suppress shock-wave effects on the electron neutrino survival probability P_+^H . For smaller values of $\sin^2 \theta_{13}$, fluctuation effects appear

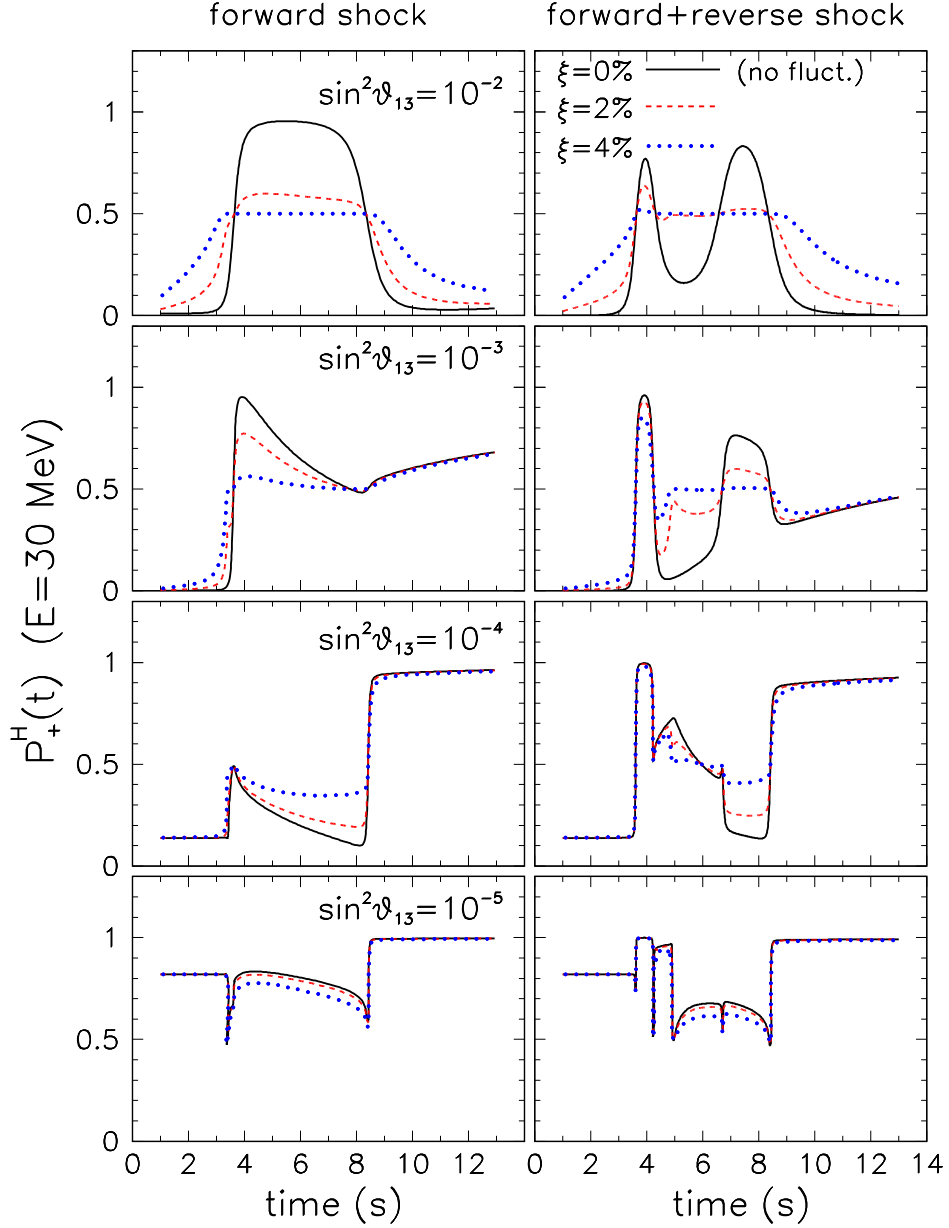


Figure 2. Probability function $P_+^H(t)$ (relevant for ν in NH or $\bar{\nu}$ in IH) at $E = 30$ MeV, for four representative values of $\sin^2 \theta_{13}$, in the presence of density fluctuations with fractional amplitude ξ equal to 0% (solid curves), 2% (dashed curves) and 4% (dotted curves). Left panels: forward shock only. Right panels: forward plus reverse shock.

to be less dangerous, but unfortunately the overall effect of shock waves on P_+^H is also small.

Figure 3 shows the time evolution of the survival probability P_-^H (relevant for ν in IH or $\bar{\nu}$ in NH, where $P_c = 0$),

$$P_-^H \simeq \frac{1}{2} \left(1 + e^{-\Gamma_-} \cos 2\theta_{13} \right) , \quad (22)$$

in the same format of Fig. 2. In the absence of matter fluctuations ($\xi = 0$), it is $\Gamma_- = 0$

and $P_-^H \simeq 1$ trivially (being $\cos 2\theta_{13} \simeq 1$ in all cases shown in Fig. 3). In the presence of fluctuations, the damping term $e^{-\Gamma_-}$ tends to lower P_-^H (down to the plateau value $1/2$ for large Γ_-). However, the relative variations of the function P_-^H in Fig. 3 are not as strong as for P_+^H in Fig. 2, since the integrand in Γ_- is never “resonant”, as it happens instead for Γ_+ . For small θ_{13} , it is simply

$$\Gamma_- \simeq \sin^2 2\theta_{13} \int_{x_0}^{x_s} \frac{\mathcal{D}(x)}{(1 + V(x)/k_H)^2} dx, \quad (23)$$

namely, the damping factor Γ_- decreases with $\sim \theta_{13}^2$, and its effect vanishes more rapidly than for Γ_+ . This fact explains why, in Fig. 3, fluctuation effects are visible only at larger values of θ_{13} (upper panels, $\sin^2 \theta_{13} = 10^{-2}$) as compared with Fig. 2. The absence of level crossing effects in P_-^H strongly reduces the sensitivity to the details of the shock-wave profile, so that for $\xi > 0$ there is hardly any difference between the left and right upper panels in Fig. 3.

From the previous discussion, stochastic density fluctuations appear to be most relevant in the cases where P_+^H (rather than P_-^H) is involved, i.e., neutrinos in normal hierarchy or antineutrinos in inverted hierarchy. For this reason, in the next section we shall examine the impact of these results in a phenomenologically relevant case ($\bar{\nu}$ in IH), by calculating observable spectra of positrons induced by $\bar{\nu}_e$ through inverse beta decay.

Finally, we comment about the effects of fluctuations on the survival probability P_{ee}^L in the “low” (L) subsystem. In the presence of density fluctuations, this probability can be calculated as

$$P_{ee}^L \simeq \frac{1}{2} \mp \frac{1}{2} e^{-\Gamma_{\pm}(L)} \cos 2\theta_{12}, \quad (24)$$

which is analogous to Eq. (17) for the adiabatic case $P_c = 0$ (the adiabaticity of the L subsystem is discussed in [8]). The damping integral in the above equations reads

$$\Gamma_{\pm}(L) = \int_{x_0}^{x_s} \mathcal{D}(x) \sin^2 2\tilde{\theta}_{12}^{\pm}(x) dx, \quad (25)$$

where the definition of $\tilde{\theta}_{12}^{\pm}$ is analogous to that in Eq. (11), but in terms of θ_{12} and of $k_L = \delta m^2/2E$. Since k_L is a factor ~ 30 smaller than k_H , one has typically $V/k_L \gg 1$ for $x < x_s$, and thus $\sin^2 2\tilde{\theta}_{12}(x) \ll 1$ in Eq. (25), except possibly at late times ($t \gtrsim 10$ s, see Fig. 1), where the crossing condition $V \simeq k_L$ can be realized, leading to $\sin^2 \tilde{\theta}_{12} \simeq 1$ for *neutrinos*. However, at late times the neutrino luminosity is also small. Therefore, the damping effects of $\Gamma_{\pm}(L)$ are either small or suppressed by a low luminosity, and can be safely neglected for the purposes of our work. One can simply take $e^{-\Gamma_{\pm}(L)} \simeq 1$ in Eq. (24), thus recovering Eq. (4).

4. Observable positron spectra from SN $\bar{\nu}$ in inverted hierarchy

As an application of the previous results, we study the effects of stochastic matter fluctuations on the observable positron time spectra detectable through the inverse

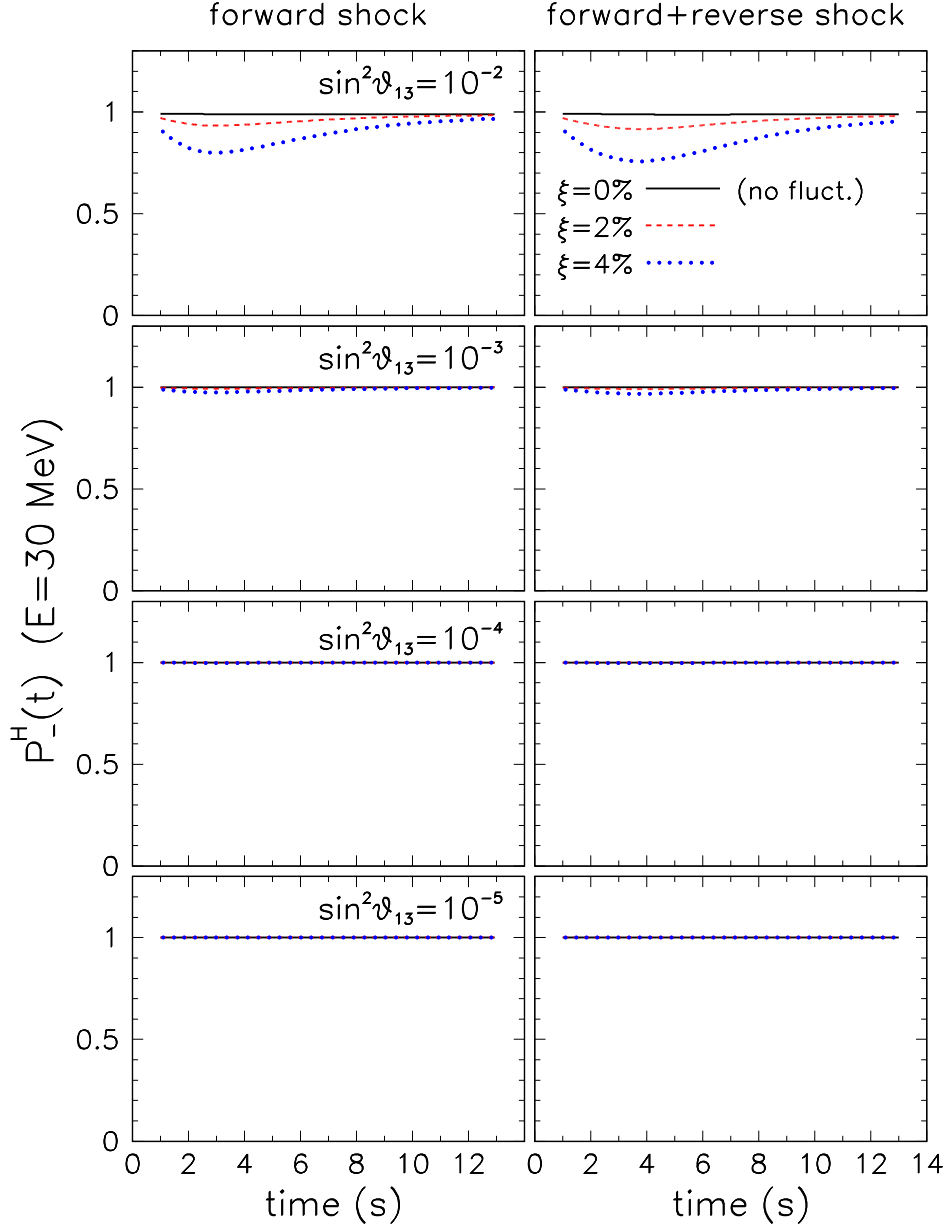


Figure 3. As in Fig. 2, but for the probability function $P_-^H(t)$ (relevant for ν in IH or $\bar{\nu}$ in NH).

beta-decay reaction

$$\bar{\nu}_e + p \rightarrow n + e^+ , \quad (26)$$

which represents the main SN neutrino detection channel in present [45] and planned Cherenkov detectors [46–49], as well as in scintillation detectors [50–52]. Therefore, in this Section we focus on electron antineutrinos, in the relevant case of inverted hierarchy,⁺ where shock-wave (plus fluctuation) effects become potentially observable

⁺ An analogous study (not presented here) could be performed for the neutrino channel in normal hierarchy, in the context of ν_e -sensitive detectors, such as liquid argon time proportional chambers [53].

through the H subsystem dynamics,

$$P_{ee} \simeq \cos^2 \theta_{12} P_+^H. \quad (27)$$

Positron event rates are calculated for a reference 0.4 Mton water-Cherenkov detector, with neutrino spectra at the supernova source, interaction cross sections, and detection parameters fixed as in our previous work [12], to which the reader is referred for further details. Here we just mention that in [12] two representative “low” and “high” positron energy bins (at $E_{\text{pos}} = 20 \pm 5$ and 45 ± 5 MeV, respectively) were identified as good relative tracers of shock-wave effects. Indeed, as discussed in [12] (for no fluctuations), the time spectra at relatively high energy ($E_{\text{pos}} = 45 \pm 5$ MeV) show strong signatures of the shock-wave propagation, especially for increasing $\sin^2 \theta_{13}$, through nonmonotonic time variations of the event rates. Conversely, the shock-induced time variations in the bin $E_{\text{pos}} = 20 \pm 5$ MeV are significantly smaller; at such energy, in fact, the initial electron and non-electron antineutrino fluxes (as used in our calculation input) happen to be approximatively equal, and the effects of flavor transitions largely cancel.

Figure 4 shows absolute time spectra of events within the two reference positron energy bins ($E_{\text{pos}} = 20 \pm 5$ MeV and $E_{\text{pos}} = 45 \pm 5$ MeV) for four representative values of $\sin^2 \theta_{13}$, and for both $\xi = 0$ (no fluctuations, solid histograms) and $\xi = 4\%$ (dashed histograms). The left and right panels refer to the case of forward shock only and of forward plus reverse shock, respectively. In the presence of stochastic density fluctuations ($\xi = 4\%$ in Fig. 4), the spectra for the low-energy positron bin are basically unaffected, since all flavor transition effects (modified or not by fluctuations) are small. The time spectra for the high-energy positron bin ($E_{\text{pos}} = 45 \pm 5$ MeV) are instead significantly smoothed out by fluctuation effects for $\sin^2 \theta_{13} \gtrsim \mathcal{O}(10^{-3})$, as expected from the discussion of Fig. 2. Therefore, even at small amplitude ($\xi = 4\%$), fluctuations can suppress the shock imprint on the time spectra, and make them qualitatively similar to those in normal hierarchy (where they are expected a priori to be smooth and monotonic).

As suggested in [12] (for the case of no fluctuations), the relative flavor transition effects at low and high energy are best displayed by showing the ratio of the spectra at 20 ± 5 MeV and 45 ± 5 MeV, where the first spectrum acts as a “normalization” factor. Figure 5 shows such ratio (in inverted hierarchy) for the same values of ξ and $\sin^2 \theta_{13}$ of Fig. 4. In the absence of stochastic fluctuations ($\xi = 0$), we recover the fact [12] that the spectral ratio can track the time variations of the electron antineutrino survival probability P_+^H , as evident from a visual comparison of the solid curves ($\xi = 0$) in Figs. 2 and 5.* Unfortunately, stochastic density fluctuations (dashed curves with $\xi = 4\%$ in Fig. 5) destroy this nice correspondence for $\sin^2 \theta_{13} \gtrsim \mathcal{O}(10^{-3})$. The spectral ratio becomes smoother, and the “peaks and valleys” induced by the shock wave on P_+^H disappear. The damping effect implies a net loss of information about the shock wave

* The analysis in [12] actually refers to the crossing probability P_c . However, in the absence of fluctuations, the smallness of θ_{13} implies that $P_+^H \approx P_c$, see Eq. (10).

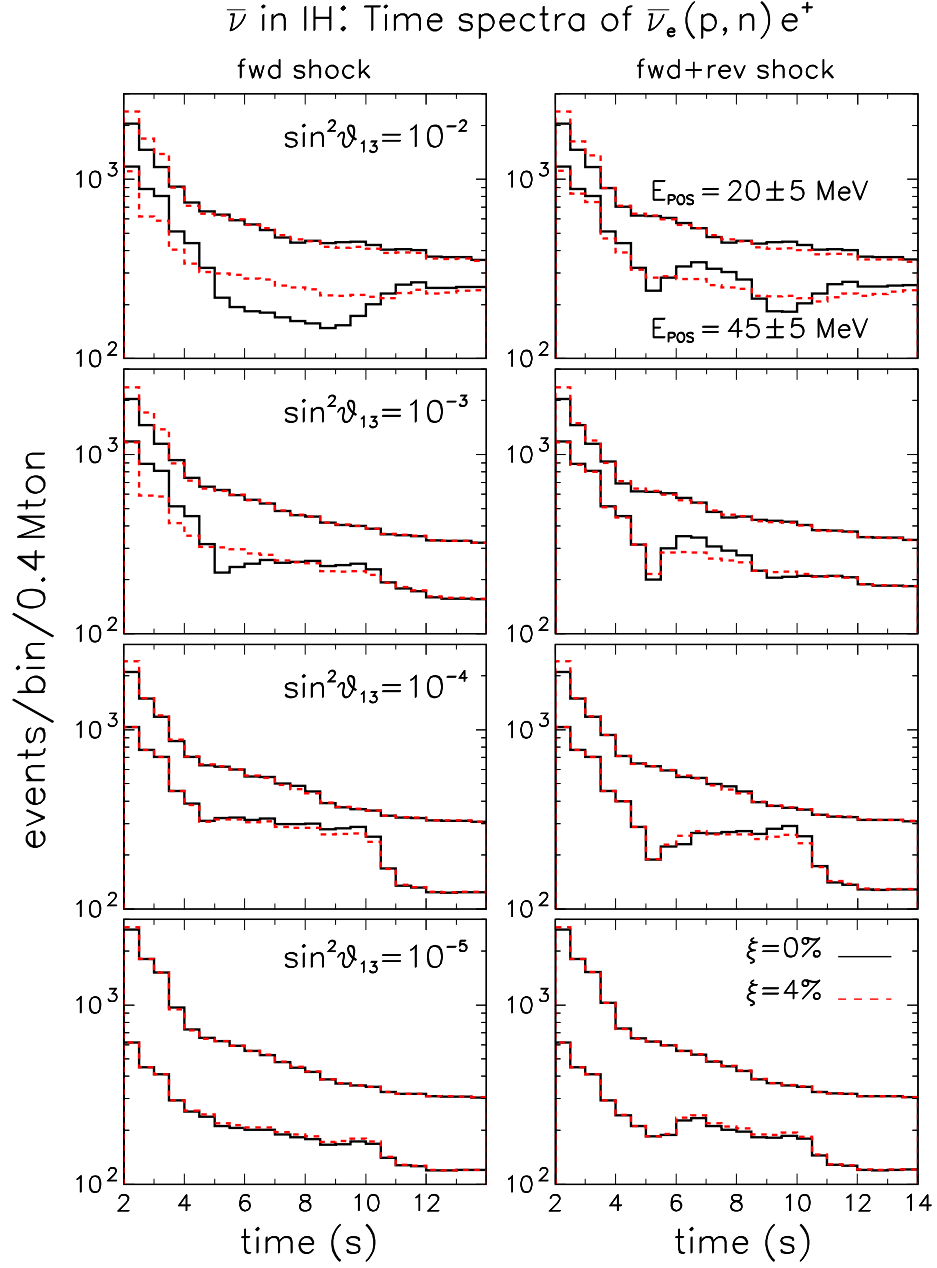


Figure 4. Absolute time spectra of positron events induced by $\bar{\nu}_e$ in IH in a 0.4 Mton water-Cherenkov detector, in the presence of forward shock (left panels) and forward plus reverse shock (right panels). Four representative values of $\sin^2 \theta_{13}$ are considered. The solid histograms refer to the case of no fluctuation ($\xi = 0$), while the dashed ones refer to the case of fluctuations with $\xi = 4\%$. In each panel, the upper (lower) couple of histograms refers to the positron energy bin $E_{\text{pos}} = 20 \pm 5$ MeV ($E_{\text{pos}} = 45 \pm 5$ MeV).

in the observable neutrino spectra.

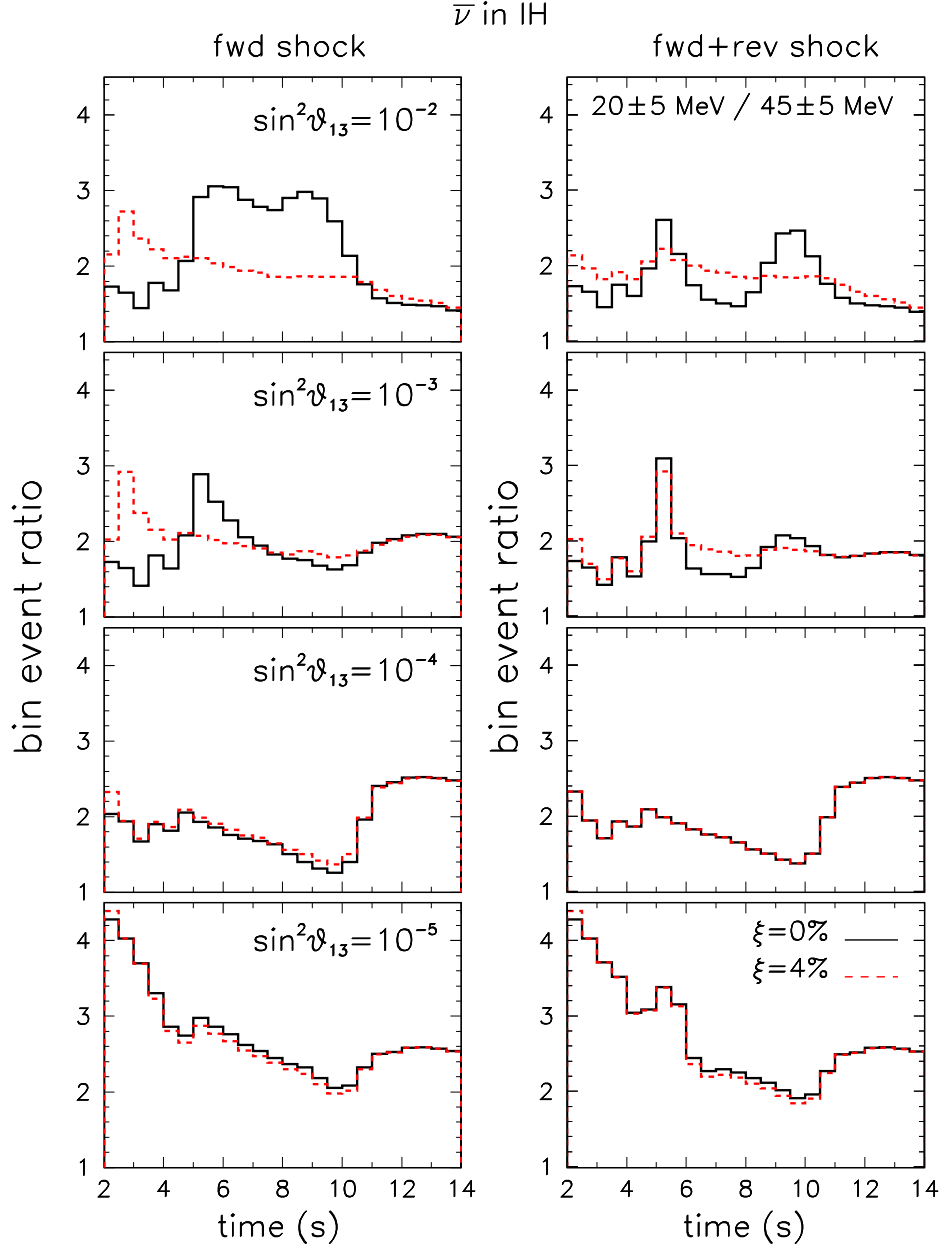


Figure 5. Time dependence of the ratio of events between the energy bins $E_{\text{pos}} = 20 \pm 5$ MeV and $E_{\text{pos}} = 45 \pm 5$ MeV in the case of forward shock only (left panels) and forward plus reverse shock (right panels). The ratio refers to $\bar{\nu}_e$ in inverted hierarchy for no fluctuation ($\xi = 0$, solid curves) and a fluctuation amplitude $\xi = 4\%$ of the local matter potential (dashed curves).

5. Summary and conclusions

Stochastic density fluctuations in supernova matter may produce observable effects on the supernova neutrino signal. In this context, previous works have been focussed on static and monotonic profiles. In this paper, we have investigated the case of time-dependent and non-monotonic profiles, embedding forward (plus reverse) shock

propagation, as suggested by recent SN numerical simulations. In the hypothesis of small-scale ($L_0 \sim \mathcal{O}(10 \text{ km})$) and small-amplitude ($\xi \lesssim \text{few\%}$) fluctuations, we have discussed an analytical recipe to evaluate the SN electron (anti)neutrino survival probability P_{ee} , which accounts for both standard matter transitions and additional “flavor-depolarization” effects induced by the fluctuations, and which accurately reproduces the numerical results (see the Appendix).

We find that, stochastic fluctuations—possibly arising after the shock front passage—may significantly suppress the imprint of SN shock waves on P_{ee} in the time domain, the more the larger $\sin^2 \theta_{13}$. For decreasing $\sin^2 \theta_{13}$, fluctuation effects decrease, but shock-wave signatures also become less pronounced. An application to observable time spectra of positron events in large water-Cherenkov detectors shows that, for the phenomenologically relevant case of inverted hierarchy, the time spectra can easily lose any imprint of the shock wave for $\sin^2 \theta_{13} \gtrsim \mathcal{O}(10^{-3})$. Therefore, in the presence of stochastic fluctuations, it might be difficult to “monitor” the shock-wave in real time in a future galactic SN explosion, or to find unmistakable signatures of inverted mass hierarchy effects.

In this context, future work might include a “fluctuation analysis” of the SN 1987A neutrino events [54] and of the expected supernova relic neutrino spectrum [55–57]. For instance, some studies of the SN 1987A $\bar{\nu}_e$ in the case of inverted hierarchy [58] found a tension between data and theory in the case of adiabatic transitions (i.e., $\sin^2 \theta_{13} \gtrsim 10^{-4}$) and inverted hierarchy, using a static SN profile. The effect of both nonadiabatic crossings and of damping behind the shock front might put these results in a different perspective.

In any case, further studies will greatly benefit from improvements of numerical SN simulations, so as to follow the shock wave evolution with much higher space-time resolution than currently possible. A better theoretical understanding of the possibility and property of stochastic density fluctuations in the SN envelope might also help to remove the simplifying assumptions adopted in this work.

Acknowledgments

This work is supported in part by the Italian “Istituto Nazionale di Fisica Nucleare” (INFN) and by the “Ministero dell’Istruzione, Università e Ricerca” (MIUR) through the “Astroparticle Physics” research project.

Appendix A. Stochastic neutrino master equation: analytical and numerical solutions

For the sake of completeness, in this Appendix we explicitly derive Eq. (17) (based on previous literature on the subject) and compare it with our numerical results for representative SN shock-wave cases. To avoid an excessive “ \pm ” notation, we consider here only the case of neutrinos in normal hierarchy. The cases of antineutrinos and

of inverted hierarchy are obtained by the replacements $V \rightarrow -V$ and $k_H \rightarrow -k_H$, respectively.

In the presence of stochastic matter fluctuations, one must consider the neutrino evolution within a statistical ensemble of density profiles. Averaging over the ensemble generally produces a loss of the coherence in the system. In this context, the appropriate formalism involves the neutrino density matrix ρ .

For a 2ν mixing problem (as in the H subsystem), the density matrix in the flavor basis $(\nu_e, \nu_a)^T$, where ν_a is any linear combination of ν_μ and ν_τ , can be expressed in terms of a “polarization vector” \mathbf{P} [59–62]:

$$\rho = \frac{1}{2}(1 + \mathbf{P} \cdot \boldsymbol{\sigma}) , \quad (\text{A.1})$$

where

$$\mathbf{P} = \begin{pmatrix} 2\text{Re}(\nu_e^* \nu_a) \\ 2\text{Im}(\nu_e^* \nu_a) \\ 2|\nu_e|^2 - 1 \end{pmatrix} , \quad (\text{A.2})$$

and $\boldsymbol{\sigma}$ is the vector of Pauli matrices. The length $|\mathbf{P}|$ of the polarization vector ($|\mathbf{P}|^2 = \text{Tr}\rho^2$) measures the degree of coherence of the system: $|\mathbf{P}| = 1$ corresponds to a pure state, $0 < |\mathbf{P}| < 1$ to a partially mixed state, and $|\mathbf{P}| = 0$ to a completely mixed state.

With or without fluctuations, the Hamiltonian for neutrinos propagating in matter in the “high” subsystem is the usual one [37]:

$$H \equiv \frac{1}{2}\mathbf{h} \cdot \boldsymbol{\sigma} = \frac{1}{2}[k_H \sin 2\theta_{13}] \sigma_1 + \frac{1}{2}[V(x) - k_H \cos 2\theta_{13}] \sigma_3 , \quad (\text{A.3})$$

with

$$\mathbf{h} = (k_H \sin 2\theta_{13}, \ 0, \ V(x) - k_H \cos 2\theta_{13}) . \quad (\text{A.4})$$

In the presence of stochastic matter density fluctuations, the potential has been expressed as $V(x) = V_0(x)[1 + \xi(x)]$, with δ -correlated Gaussian fluctuations (see Sec. 3.1). In this case, the Liouville evolution of the fluctuations-averaged density matrix reads [20–22]‡

$$\frac{d}{dx}\rho = -i[H_0, \rho] - \frac{1}{4}\mathcal{D}[\sigma_3, [\sigma_3, \rho]] , \quad (\text{A.5})$$

where H_0 is the unperturbed Hamiltonian (for $\xi = 0$) and \mathcal{D} is the same damping parameter as in Eq. (19).

Equation (A.5) has the well-known Lindblad form for dissipative systems [63], where the first term in the right-hand side reproduces the standard Liouville equation for the ν density matrix, while the second term violates the conservation of $\text{Tr}\rho^2$ and allows transitions from pure to mixed states. In terms of the polarization vector, Eq. (A.5) assumes the neat form of a Bloch equation [60, 65]

$$\frac{d}{dx}\mathbf{P} = \mathbf{h}_0 \times \mathbf{P} - \mathcal{D}\mathbf{P}_T , \quad (\text{A.6})$$

‡ For neutrinos propagating in a stochastic matter, the density matrix [Eq. (A.1)] and the polarization vector [Eq. (A.2)] must be understood as averaged over the ensemble of density profiles.

where \mathbf{h}_0 corresponds to Eq. (A.4) with $\xi = 0$, and $\mathbf{P}_T = \mathbf{P} - \mathbf{P}_3$ is the “transverse” part of the polarization vector. In this picture, the first term in the right hand side represents the usual coherent “precession” of the polarization vector \mathbf{P} around the vector \mathbf{h}_0 [59–62, 64], while the second (damping) term produces a loss of coherence, i.e., a shortening of the vector length $|\mathbf{P}|$ [60, 65].

Using Eqs. (A.2)–(A.4), one can write Eq. (A.6) in components [20–24]

$$\begin{aligned} \frac{d}{dx} \begin{pmatrix} P_1 \\ P_2 \\ P_3 \end{pmatrix} &= \begin{pmatrix} -\mathcal{D}(x) & -V_0(x) + k_H c_{2\theta} & 0 \\ V_0(x) - k_H c_{2\theta} & -\mathcal{D}(x) & -k_H s_{2\theta} \\ 0 & k_H s_{2\theta} & 0 \end{pmatrix} \begin{pmatrix} P_1 \\ P_2 \\ P_3 \end{pmatrix} \\ &\equiv \mathcal{K} \begin{pmatrix} P_1 \\ P_2 \\ P_3 \end{pmatrix}, \end{aligned} \quad (\text{A.7})$$

where $c_{2\theta} \equiv \cos 2\theta_{13}$ and $s_{2\theta} \equiv \sin 2\theta_{13}$. The (fluctuation-averaged) survival probability for electron neutrinos $\nu = (1, 0)^T$ is then given by

$$P_+^H = \text{Tr}[\rho \nu^\dagger \nu] = \frac{1 + P_3}{2}. \quad (\text{A.8})$$

In general, the system of equations [Eq. (A.7)] has to be solved numerically, as done e.g. in [20, 21, 23]. However, in the case of small-amplitude fluctuations, the damping term \mathcal{D} in Eq. (A.7) can be treated as a perturbation. In this way, it is possible to integrate analytically Eq. (A.7). Here we closely follow the derivation presented in [24].

We start by diagonalizing the \mathcal{K} matrix in Eq. (A.7) at 0-th order in \mathcal{D} , establishing the “instantaneous diagonal basis”

$$\begin{pmatrix} \tilde{P}_1 \\ \tilde{P}_2 \\ \tilde{P}_3 \end{pmatrix} = \mathcal{U} \begin{pmatrix} P_1 \\ P_2 \\ P_3 \end{pmatrix}. \quad (\text{A.9})$$

The matrix $\mathcal{U} = [\hat{\mathbf{u}}_1, \hat{\mathbf{u}}_2, \hat{\mathbf{u}}_0]$ diagonalizes \mathcal{K} as

$$\mathcal{K}_d = \text{diag}(\lambda_1, \lambda_2, \lambda_0) = \mathcal{U} \mathcal{K} \mathcal{U}^\dagger, \quad (\text{A.10})$$

where the three eigenvalues are

$$\lambda_0 = 0, \quad (\text{A.11})$$

$$\lambda_{1,2} = \pm i |\mathbf{h}_0| = \pm i \sqrt{(k_H \cos 2\theta_{13} - V)^2 + (k_H \sin 2\theta_{13})^2}, \quad (\text{A.12})$$

and the corresponding eigenvectors are

$$\hat{\mathbf{u}}_0 = \hat{\mathbf{h}}_0, \quad (\text{A.13})$$

$$\hat{\mathbf{u}}_{1,2} = \frac{1}{\sqrt{2}} (\hat{\mathbf{h}}_0 \times \hat{\mathbf{s}} \pm i \hat{\mathbf{s}}), \quad (\text{A.14})$$

with $\hat{\mathbf{h}}_0 = \mathbf{h}_0/|\mathbf{h}_0|$, while $\hat{\mathbf{s}}$ is an arbitrary unitary vector perpendicular to \mathbf{h}_0 . By choosing $\hat{\mathbf{s}} = (0, 1, 0)$, one obtains

$$\hat{\mathbf{u}}_0 = \begin{pmatrix} \sin 2\tilde{\theta}_{13}^+ \\ 0 \\ -\cos 2\tilde{\theta}_{13}^+ \end{pmatrix}, \hat{\mathbf{u}}_1 = \frac{1}{\sqrt{2}} \begin{pmatrix} \cos 2\tilde{\theta}_{13}^+ \\ i \\ \sin 2\tilde{\theta}_{13}^+ \end{pmatrix}, \hat{\mathbf{u}}_2 = \frac{1}{\sqrt{2}} \begin{pmatrix} \cos 2\tilde{\theta}_{13}^+ \\ -i \\ \sin 2\tilde{\theta}_{13}^+ \end{pmatrix} \quad (\text{A.15})$$

while the matrix \mathcal{U} takes the form

$$\mathcal{U} = \begin{bmatrix} \frac{1}{\sqrt{2}} \cos 2\tilde{\theta}_{13}^+ & \frac{1}{\sqrt{2}} \cos 2\tilde{\theta}_{13}^+ & \sin 2\tilde{\theta}_{13}^+ \\ \frac{i}{\sqrt{2}} & -\frac{i}{\sqrt{2}} & 0 \\ \frac{1}{\sqrt{2}} \sin 2\tilde{\theta}_{13}^+ & \frac{1}{\sqrt{2}} \sin 2\tilde{\theta}_{13}^+ & -\cos 2\tilde{\theta}_{13}^+ \end{bmatrix}, \quad (\text{A.16})$$

where $\tilde{\theta}_{13}^+$ is the mixing angle in matter defined by

$$\sin 2\tilde{\theta}_{13}^+ = \frac{\sin 2\theta_{13}}{\sqrt{(\cos 2\theta_{13} - V/k_H)^2 + (\sin 2\theta_{13})^2}}, \quad (\text{A.17})$$

$$\cos 2\tilde{\theta}_{13}^+ = \frac{\cos 2\theta_{13} - V/k_H}{\sqrt{(\cos 2\theta_{13} - V/k_H)^2 + (\sin 2\theta_{13})^2}}. \quad (\text{A.18})$$

In the diagonal basis, Eq. (A.7) becomes

$$\frac{d}{dx} \tilde{P} = \mathcal{K}_d \tilde{P} - \mathcal{U} \frac{d\mathcal{U}^\dagger}{dx} \tilde{P}. \quad (\text{A.19})$$

We assume that the propagation is adiabatic ($d\mathcal{U}^\dagger/dx = 0$), except near one “crossing point” x_c where $V(x_c) \simeq k_H$ (The generalization to multiple crossings is straightforward). In this approximation, Eq. (A.19) has thus a formal solution:

$$\mathbf{P}(x) = \mathcal{U}^\dagger(x) \mathcal{S}(x_c, x) \mathcal{Q}(x_c) \mathcal{S}(x_0, x_c) \mathcal{U}(x_0) \mathbf{P}(x_0), \quad (\text{A.20})$$

where x_0 is the neutrino production point, and

$$\mathcal{S}(x_1, x_2) = \text{diag} [e^{i\phi(x_1, x_2)}, e^{-i\phi(x_1, x_2)}, 1], \quad (\text{A.21})$$

is the adiabatic evolution operator, while $\phi(x_1, x_2) = \int_{x_1}^{x_2} dy |\mathbf{h}_0(y)|$, and the non-diagonal operator $\mathcal{Q}(x_c)$ takes into account the nonadiabatic transition (level crossing) around the point x_c .

By inserting the above expressions in Eq. (A.8), and averaging over the oscillatory terms, one gets:

$$P_+^H = \frac{1 + [\mathcal{Q}(x_c)]_{33} \cos 2\tilde{\theta}_{13}^+(x) \cos 2\tilde{\theta}_{13}^+(x_0)}{2}, \quad (\text{A.22})$$

The comparison of Eq. (A.22) with Eq. (10) leads to the identification $[\mathcal{Q}(x_c)]_{33} = 1 - 2P_c$, where P_c is the crossing probability between the two mass eigenstates in matter. At 0-th order in \mathcal{D} one thus recovers the usual (no-fluctuation) Parke’s formula:

$$P_+^H = \frac{1}{2} + \left(\frac{1}{2} - P_c \right) \cos 2\tilde{\theta}_{13}^+(x) \cos 2\tilde{\theta}_{13}^+(x_0). \quad (\text{A.23})$$

The first-order corrections to the eigenvalues [Eqs. (A.11)–(A.12)] and eigenvectors [Eqs. (A.13)–(A.14)] are calculated through the standard perturbation theory as:

$$\lambda_a^{(1)} = \lambda_a + \delta\lambda_a = \lambda_a - \mathcal{D} \hat{\mathbf{u}}_a^\dagger \mathcal{G} \hat{\mathbf{u}}_a, \quad (\text{A.24})$$

$$\hat{\mathbf{u}}_a^{(1)} = \hat{\mathbf{u}}_a + \delta\hat{\mathbf{u}}_a = \hat{\mathbf{u}}_a - \mathcal{D} \sum_{b \neq a} \frac{\hat{\mathbf{u}}_b^\dagger \mathcal{G} \hat{\mathbf{u}}_a}{\lambda_a - \lambda_b} \hat{\mathbf{u}}_b, \quad (\text{A.25})$$

where $a, b = 0, 1, 2$ and $\mathcal{G} = \text{diag}(1, 1, 0)$. Since $\hat{\mathbf{u}}_b^\dagger \mathcal{G} \hat{\mathbf{u}}_a = \delta_{ab} - (\hat{\mathbf{u}}_a)_3 (\hat{\mathbf{u}}_b)_3$, one obtains

$$\begin{aligned} \lambda_0' &= -\mathcal{D} \sin^2 2\tilde{\theta}_{13}^+ \\ \lambda_{1,2}' &= \pm i|\mathbf{h}_0| - \mathcal{D} \left(1 - \frac{1}{2} \sin^2 2\tilde{\theta}_{13}^+ \right), \end{aligned} \quad (\text{A.26})$$

and

$$\begin{aligned}\hat{\mathbf{u}}_0^{(\prime)} &= \hat{\mathbf{u}}_0 + \mathcal{D} \frac{\sin 2\tilde{\theta}_{13}^+ \cos 2\tilde{\theta}_{13}^+}{|\mathbf{h}_0|} \hat{\mathbf{s}} , \\ \hat{\mathbf{u}}_{1,2}^{(\prime)} &= \hat{\mathbf{u}}_{1,2} \mp i\mathcal{D} \frac{\sin 2\tilde{\theta}_{13}^+}{\sqrt{2}|\mathbf{h}_0|} \left[-\cos 2\tilde{\theta}_{13}^+ \hat{\mathbf{u}}_0 + \frac{\sin 2\tilde{\theta}_{13}^+}{2\sqrt{2}} \hat{\mathbf{u}}_{2,1} \right] .\end{aligned}\quad (\text{A.27})$$

By substituting the first-order eigenvalues in Eq. (A.20), the matrix $\mathcal{S}(x_1, x_2)$ can be rewritten as:

$$\mathcal{S}(x_1, x_2) = \text{diag} \left[e^{i\phi(x_1, x_2) + \int_{x_1}^{x_2} dx \delta\lambda_1}, e^{-i\phi(x_1, x_2) + \int_{x_1}^{x_2} dx \delta\lambda_2}, e^{+ \int_{x_1}^{x_2} dx \delta\lambda_0} \right] . (\text{A.28})$$

The expressions of $\delta\lambda_{1,2}$ are irrelevant for our purposes, since they disappear after averaging over the oscillating terms in P_+^H . Notice that, in Eq. (A.20), only the operator \mathcal{S} is corrected at first order. The matrix $\mathcal{U}(x_0)$ remains unchanged, since the high-density condition $V(x_0)/k_H \gg 1$ implies that $\sin 2\tilde{\theta}_{13}^+(x_0) \simeq 0$ in Eq. (A.27). The matrix $\mathcal{U}(x)$ at the detection point is also unchanged, since $\tilde{\theta}_{13}^+(x) = \theta_{13}$ and $\mathcal{D} = 0$ at the Earth.

Finally, for small fluctuations, we assume that the operator $\mathcal{Q}(x_c)$ (which only depends on the crossing condition $V(x_c) \simeq k_H$) is unchanged. After averaging on the oscillating terms one then obtains

$$P_+^H \simeq \frac{1}{2} + \left(\frac{1}{2} - P_c \right) e^{-\Gamma_+} \cos 2\tilde{\theta}_{13}^+(x) \cos 2\tilde{\theta}_{13}^+(x_0) , \quad (\text{A.29})$$

where

$$\Gamma_+ = \int_{x_0}^x dy \lambda'_0(y) = \int_{x_0}^x dy \mathcal{D}(y) \sin^2 2\tilde{\theta}_{13}^+(y) . \quad (\text{A.30})$$

In the case of detected supernova neutrinos, $\tilde{\theta}_{13}^+(x)$ corresponds to the vacuum value θ_{13} , while the initial high-density condition implies $\cos 2\tilde{\theta}_{13}^+(x_0) \simeq -1$. With these positions, Eq. (A.29) gives the desired expression

$$P_+^H \simeq \frac{1}{2} - \left(\frac{1}{2} - P_c \right) e^{-\Gamma_+} \cos 2\theta_{13} . \quad (\text{A.31})$$

In order to check the reliability of the analytical approximation of P_+^H in Eq. (A.31), we have compared it with the results of a numerical (Runge-Kutta) evolution of neutrino master equation [Eq. (A.7)] along representative fluctuating shock-wave profiles. Figure A1 shows our calculation of $P_+^H(t)$ at fixed neutrino energy ($E = 30$ MeV) for $\sin^2 \theta_{13} = 10^{-2}$, and for two representative fluctuation amplitudes, $\xi = 2\%$ (upper panels) and $\xi = 4\%$ (lower panels). We consider both the case of forward shock only (left panels) and forward plus reverse shock (right panels). It can be seen that the analytical calculations (solid curves) and the numerical Runge-Kutta calculations (dashed curves) are in very good agreement in the whole time interval $t \in [1, 13]$ s. The results of Figure A1 (and of other checks that we have performed for different values of $\sin^2 \theta_{13}$ and of the neutrino energy) show that the analytical calculation of P_+^H reproduces the numerical results with high accuracy. The same reassuring check has been performed also in the case of P_-^H (not shown).

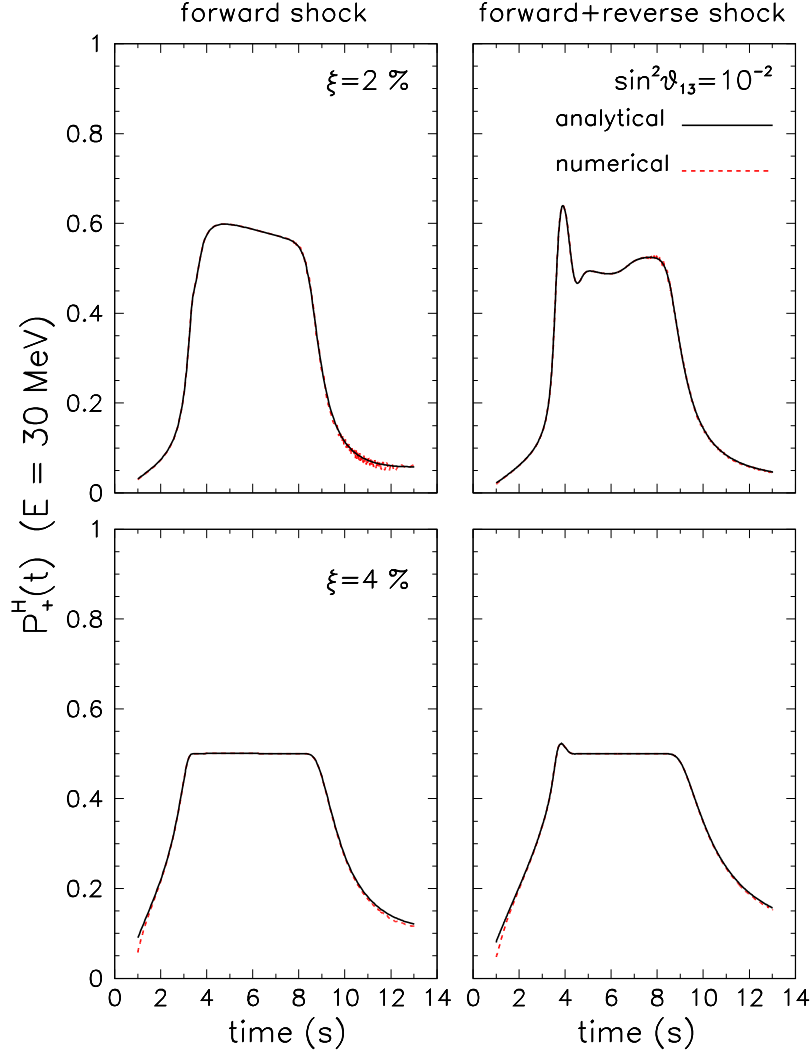


Figure A1. Comparison of analytical and numerical calculations of the electron neutrino survival probability P_+^H in the H subsystem (solid and dashed curves, respectively) for $E = 30$ MeV, $\sin^2 \theta_{13} = 10^{-2}$, and fluctuations with amplitude $\xi = 2\%$ (upper panels) and $\xi = 4\%$ (lower panels). The left panels refer to the case of forward shock only, while the right panels to the case of forward plus reverse shock.

References

- [1] K. Kotake, K. Sato and K. Takahashi, “Explosion Mechanism, Neutrino Burst, and Gravitational Wave in Core-Collapse Supernovae,” Rept. Prog. Phys. **69**, 971 (2006) [astro-ph/0509456].
- [2] G. G. Raffelt, “Supernova neutrino oscillations,” in the Proceedings of *Nobel Symposium 2004*, Neutrino Physics (Haga Slott, Enköping, Sweden, 2004), Phys. Scripta **T121**, 102 (2005) [hep-ph/0501049].
- [3] A. Dighe, “Supernova neutrinos: Production, propagation and oscillations,” in the Proceedings of *Neutrino 2004*, 21st International Conference on Neutrino Physics and Astrophysics (Paris, France, 14-19 Jun 2004), Nucl. Phys. Proc. Suppl. **143**, 449 (2005) [hep-ph/0409268].
- [4] F. Cavanna, M. L. Costantini, O. Palamara and F. Vissani, “Neutrinos as astrophysical probes,” Surveys High Energ. Phys. **19**, 35 (2004) [astro-ph/0311256].
- [5] R. C. Schirato and G. M. Fuller, “Connection between supernova shocks, flavor transformation, and the neutrino signal,” astro-ph/0205390 (unpublished).
- [6] K. Takahashi, K. Sato, H. E. Dalhed and J. R. Wilson, “Shock propagation and neutrino oscillation in supernova,” Astropart. Phys. **20**, 189 (2003) [astro-ph/0212195].
- [7] C. Lunardini and A. Yu. Smirnov, “Probing the neutrino mass hierarchy and the 13-mixing with supernovae,” JCAP **0306**, 009 (2003) [hep-ph/0302033].
- [8] G. L. Fogli, E. Lisi, A. Mirizzi, and D. Montanino, “Analysis of energy- and time-dependence of supernova shock effects on neutrino crossing probabilities,” Phys. Rev. D **68**, 033005 (2003) [hep-ph/0304056].
- [9] R. Tomàs, M. Kachelrieß, G. Raffelt, A. Dighe, H. T. Janka and L. Scheck, “Neutrino signatures of supernova shock and reverse shock propagation,” JCAP **0409**, 015 (2004) [astro-ph/0407132].
- [10] S. Kawagoe, “Shock Wave Propagation in Prompt Supernova Explosion and the MSW Effect of Neutrino,” talk at *TAUP 2005*, 9th International Conference on Topics in Astroparticle and Underground Physics (Zaragoza, Spain, 2005), available at www.unizar.es/taup2005/talks.htm.
- [11] B. Dasgupta and A. Dighe, “Phase effects in neutrino conversions during a supernova shock wave,” hep-ph/0510219.
- [12] G. L. Fogli, E. Lisi, A. Mirizzi and D. Montanino, “Probing supernova shock waves and neutrino flavor transitions in next-generation water-Cherenkov detectors,” JCAP **0504**, 002 (2005) [hep-ph/0412046].
- [13] V. Barger, P. Huber and D. Marfatia, “Supernova neutrinos can tell us the neutrino mass hierarchy independently of flux models,” Phys. Lett. B **617**, 167 (2005) [hep-ph/0501184].
- [14] S. Choubey, N. P. Harries and G. G. Ross, “Probing neutrino oscillations from supernovae shock waves via the IceCube detector,” hep-ph/0605255.
- [15] W. Keil, H. T. Janka and E. Muller, “Ledoux-convection in protoneutron stars: A clue to supernova nucleosynthesis?,” Astrophys. Journ. **473**, L111 (1996) [astro-ph/9610203].
- [16] K. Kifonidis, T. Plewa, H. T. Janka and E. Mueller, “Non-spherical core collapse supernovae. I: Neutrino-driven convection, Rayleigh-Taylor instabilities, and the formation and propagation of metal clumps,” Astron. Astrophys. **408**, 621 (2003) [astro-ph/0302239].
- [17] R. Buras, H. T. Janka, M. Rampp and K. Kifonidis, “Two-Dimensional Hydrodynamic Core-Collapse Supernova Simulations with Spectral Neutrino Transport II. Models for Different Progenitor Stars,” astro-ph/0512189.
- [18] L. Scheck, K. Kifonidis, H. T. Janka and E. Mueller, “Multidimensional Supernova Simulations with Approximative Neutrino Transport I. Neutron Star Kicks and the Anisotropy of Neutrino-Driven Explosions in Two Spatial Dimensions,” astro-ph/0601302.
- [19] R. F. Sawyer, “Neutrino oscillations in inhomogeneous matter,” Phys. Rev. D **42**, 3908 (1990).
- [20] F. N. Loreti and A. B. Balantekin, “Neutrino oscillations in noisy media,” Phys. Rev. D **50**, 4762 (1994) [nucl-th/9406003].
- [21] A. B. Balantekin, J. M. Fetter and F. N. Loreti, “The MSW effect in a fluctuating matter density,” Phys. Rev. D **54**, 3941 (1996) [astro-ph/9604061].

- [22] F. Benatti and R. Floreanini, “Dissipative neutrino oscillations in randomly fluctuating matter,” *Phys. Rev. D* **71**, 013003 (2005) [hep-ph/0412311].
- [23] H. Nunokawa, A. Rossi, V. B. Semikoz and J. W. F. Valle, “The effect of random matter density perturbations on the MSW solution to the solar neutrino problem,” *Nucl. Phys. B* **472**, 495 (1996) [hep-ph/9602307].
- [24] C. P. Burgess and D. Michaud, “Neutrino propagation in a fluctuating sun,” *Annals Phys.* **256**, 1 (1997) [hep-ph/9606295].
- [25] A. A. Bykov, M. C. Gonzalez-Garcia, C. Pena-Garay, V. Y. Popov and V. B. Semikoz, “MSW solutions to the solar neutrino problem in presence of noisy matter density fluctuations,” hep-ph/0005244.
- [26] C. Burgess, N. S. Dzhililov, M. Maltoni, T. I. Rashba, V. B. Semikoz, M. Tortola and J. W. F. Valle, “Large mixing angle oscillations as a probe of the deep solar interior,” *Astrophys. J.* **588**, L65 (2003) [hep-ph/0209094].
- [27] M. M. Guzzo, P. C. de Holanda and N. Reggiani, “Large mixing angle solution to the solar neutrino problem and random matter density perturbations,” *Phys. Lett. B* **569**, 45 (2003) [hep-ph/0303203].
- [28] A. B. Balantekin and H. Yuksel, “Do the KamLAND and solar neutrino data rule out solar density fluctuations?,” *Phys. Rev. D* **68**, 013006 (2003) [hep-ph/0303169].
- [29] F. N. Loreti, Y. Z. Qian, G. M. Fuller and A. B. Balantekin, “Effects of random density fluctuations on matter enhanced neutrino flavor transitions in supernovae and implications for supernova dynamics and nucleosynthesis,” *Phys. Rev. D* **52**, 6664 (1995) [astro-ph/9508106].
- [30] A. S. Dighe and A. Yu. Smirnov, “Identifying the neutrino mass spectrum from the neutrino burst from a supernova,” *Phys. Rev. D* **62**, 033007 (2000) [hep-ph/9907423].
- [31] G. L. Fogli, E. Lisi, D. Montanino and A. Palazzo, “Supernova neutrino oscillations: A simple analytical approach,” *Phys. Rev. D* **65**, 073008 (2002) [Erratum-ibid. *D* **66**, 039901 (2002)] [hep-ph/0111199].
- [32] G. L. Fogli, E. Lisi, A. Marrone and A. Palazzo, “Global analysis of three-flavor neutrino masses and mixings,” hep-ph/0506083; to appear in *Prog. Part. Nucl. Phys.* (2006).
- [33] M. Apollonio *et al.*, “Search for neutrino oscillations on a long base-line at the CHOOZ nuclear power station,” *Eur. Phys. J. C* **27**, 331 (2003) [hep-ex/0301017].
- [34] T. K. Kuo and J. T. Pantaleone, “Supernova Neutrinos And Their Oscillations,” *Phys. Rev. D* **37**, 298 (1988).
- [35] S. P. Mikheyev and A. Yu. Smirnov, “Resonant Neutrino Oscillations In Matter,” *Prog. Part. Nucl. Phys.* **23**, 41 (1989).
- [36] T. K. Kuo and J. T. Pantaleone, “Neutrino Oscillations In Matter,” *Rev. Mod. Phys.* **61**, 937 (1989).
- [37] L. Wolfenstein, “Neutrino Oscillations In Matter,” *Phys. Rev. D* **17**, 2369 (1978); S. P. Mikheev and A. Yu. Smirnov, “Resonance Enhancement Of Oscillations In Matter And Solar Neutrino Spectroscopy,” *Yad. Fiz.* **42**, 1441 (1985) [*Sov. J. Nucl. Phys.* **42**, 913 (1985)].
- [38] S. T. Petcov, “Exact Analytic Description Of Two Neutrino Oscillations In Matter With Exponentially Varying Density,” *Phys. Lett. B* **200**, 373 (1988).
- [39] L. D. Landau, “Zur Theorie der Energieübertragung bei Stößen” (*“On the theory of the energy transfer in collisions”*), *Phys. Z. Sowjetunion* **1**, 88 (1932); “Zur Theorie der Energieübertragung, II” (*“On the theory of the energy transfer, II”*), *Phys. Z. Sowjetunion* **2**, 46 (1932).
- [40] C. Zener, “Nonadiabatic Crossing Of Energy Levels,” *Proc. Roy. Soc. Lond. A* **137**, 696 (1932).
- [41] E. C. Stückelberg, “Theorie der unelastischen Stösse zwischen Atomen” (*“Theory of the inelastic collisions between atoms”*), *Helv. Phys. Acta* **5**, 369 (1932).
- [42] E. Majorana, “Atomi orientati in campo magnetico variabile” (*“Oriented atoms in variable magnetic field”*), *Nuovo Cimento* **9**, 43 (1932).
- [43] F. di Giacomo and E. E. Nikitin, “Majorana formula and the Landau-Zener-Stückelberg treatment of the avoided crossing problem,” *Ups. Fiz. Nauk* **175** (5), 545 (2005) [*Physics-Uspekhi* **48** (5),

- 515 (2005)].
- [44] S. J. Parke, “Nonadiabatic Level Crossing in Resonant Neutrino Oscillations,” *Phys. Rev. Lett.* **57**, 1275 (1986).
 - [45] Y. Fukuda *et al.*, “The Super-Kamiokande detector,” *Nucl. Instrum. Meth. A* **501**, 418 (2003).
 - [46] UNO official homepage: ale.physics.sunysb.edu
 - [47] C. K. Jung, “Feasibility of a next generation underground water Cherenkov detector: UNO,” hep-ex/0005046.
 - [48] K. Nakamura, “Hyper-Kamiokande: A next generation water Cherenkov detector,” *Int. J. Mod. Phys. A* **18**, 4053 (2003).
 - [49] L. Mosca, “Status of the project of a Large International Underground Laboratory at Frejus,” talk at the Villars CERN/SPSC Meeting (Villars, Switzerland, 2004), available at nuspp.in2p3.fr/Frejus. See also J. E. Campagne, M. Maltoni, M. Mezzetto and T. Schwetz, “Physics potential of the CERN-MEMPHYS neutrino oscillation project,” hep-ph/0603172.
 - [50] L. Cadonati, F. P. Calaprice and M. C. Chen, “Supernova neutrino detection in Borexino,” *Astropart. Phys.* **16**, 361 (2002) [hep-ph/0012082].
 - [51] M. Aglietta *et al.*, “The most powerful scintillator supernovae detector: LVD,” *Nuovo Cim. A* **105**, 1793 (1992).
 - [52] L. Oberauer, “Low energy neutrino physics after SNO and KamLAND,” *Mod. Phys. Lett. A* **19**, 337 (2004) [hep-ph/0402162]; L. Oberauer, “LENA,” talk at *NO-VE 2006*, 3rd International Workshop on Neutrino Oscillations in Venice (Venice, Italy, 2006), available at http://axpd24.pd.infn.it/NO-VE2006/talks/NOVE_Oberauer.ppt.
 - [53] I. Gil-Botella and A. Rubbia, “Decoupling supernova and neutrino oscillation physics with LAr TPC detectors,” *JCAP* **0408**, 001 (2004) [hep-ph/0404151].
 - [54] A. Mirizzi and G. G. Raffelt, “New analysis of the SN 1987A neutrinos with a flexible spectral shape,” *Phys. Rev. D* **72**, 063001 (2005) [astro-ph/0508612].
 - [55] M. Malek *et al.* [Super-Kamiokande Collaboration], “Search for supernova relic neutrinos at Super-Kamiokande,” *Phys. Rev. Lett.* **90**, 061101 (2003) [hep-ex/0209028].
 - [56] G. L. Fogli, E. Lisi, A. Mirizzi and D. Montanino, “Three-generation flavor transitions and decays of supernova relic neutrinos,” *Phys. Rev. D* **70**, 013001 (2004) [hep-ph/0401227].
 - [57] H. Yuksel, S. Ando and J. F. Beacom, “Direct measurement of supernova neutrino emission parameters with a gadolinium enhanced Super-Kamiokande detector,” astro-ph/0509297.
 - [58] H. Minakata and H. Nunokawa, “Inverted hierarchy of neutrino masses disfavored by supernova 1987A,” *Phys. Lett. B* **504**, 301 (2001) [hep-ph/0010240].
 - [59] S. P. Mikheyev and A. Yu. Smirnov, “Neutrino Oscillations In Matter With Varying Density,” in the Proceedings of *’86 Massive Neutrinos in Astrophysics and in Particle Physics*, Sixth Moriond Workshop (Tignes, France, 1986), edited by O. Fackler and J. Tran Thanh Van (Editions Frontières, Gif-sur-Yvette, 1986), p. 355.
 - [60] L. Stodolsky, “On The Treatment Of Neutrino Oscillations In A Thermal Environment,” *Phys. Rev. D* **36**, 2273 (1987).
 - [61] C. W. Kim, J. Kim and W. K. Sze, “On The Geometrical Representation Of Neutrino Oscillations In Vacuum And Matter,” *Phys. Rev. D* **37**, 1072 (1988).
 - [62] H. Duan, G. M. Fuller and Y. Z. Qian, “Collective neutrino flavor transformation in supernovae,” astro-ph/0511275.
 - [63] G. Lindblad, “On The Generators Of Quantum Dynamical Semigroups,” *Commun. Math. Phys.* **48**, 119 (1976).
 - [64] A. Yu. Smirnov, “Neutrino conversion and neutrino astrophysics,” hep-ph/9811296, in the Proceedings of *Symposium on New Era in Neutrino Physics* (Tokyo, Japan, 1998), published in “Tokyo 1998, New era in neutrino physics”, edited by H. Minakata and O. Yasuda, *Frontiers of Science Series n. 25* (Univ. Academy Press, Tokyo, Japan, 1999), p 1.
 - [65] G. G. Raffelt, “Stars as Laboratories for Fundamental Physics,” (Univ. of Chicago Press, Chicago, IL, 1996).